# Systematic Design of Pulse Dosing to Eradicate Persister Bacteria

**Garima Singh, Mehmet A. Orman, Jacinta C. Conrad, Michael Nikolaou***

Chemical and Biomolecular Engineering Department,
University of Houston, Houston, TX, United States

***Corresponding Author:**
nikolaou@uh.edu

**Keywords: Persister cells, pulse dosing, modeling**

---

**Abstract**

A small fraction of infectious bacteria use persistence as a strategy to survive exposure to antibiotics. Periodic pulse dosing of antibiotics has long been considered a potentially effective strategy towards eradication of persisters. Recent studies have demonstrated through *in vitro* experiments that it is indeed feasible to achieve such effectiveness. However, systematic design of periodic pulse dosing regimens to treat persisters is currently lacking. Here we rigorously develop a methodology for the systematic design of optimal periodic pulse dosing strategies for rapid eradication of persisters. A key outcome of the theoretical analysis, on which the proposed methodology is based, is that bactericidal effectiveness of periodic pulse dosing depends mainly on the ratio of durations of the corresponding on and off parts of the pulse. Simple formulas for critical and optimal values of this ratio are derived. The proposed methodology is supported by computer simulations and *in vitro* experiments.

**Author Summary**

Administering antibiotics in periodic pulses that alternate between high and low concentration has long been known as a possible dosing strategy to treat stubborn infections caused by bacteria known as *persisters*. Such bacteria use clever mechanisms to survive otherwise lethal temporary exposure to antibiotics and to resume normal activity upon antibiotic removal. Persisters pose a serious health problem. Recent studies have elucidated mechanisms of persistence and have confirmed that pulse dosing, if designed appropriately, can indeed be effective. However, effective pulse dosing design has been mainly handled by trial and error, requiring relatively extensive experimentation. Here we develop a method for rapid systematic design of effective pulse dosing. The method relies on a simple mathematical model and a minimal amount of standard experimental data. We derive corresponding design formulas that explicitly characterize the shape of generally effective or optimal periodic pulses. We tested our method through computer simulations and *in vitro* experiments, as well as on prior literature data. In all cases, the outcomes on persister bacteria eradication predicted by our method were confirmed. These results pave the way for ultimately developing effective pulse dosing regimens in realistic situations *in vivo*.

## 1 INTRODUCTION

Persister cells are a small fraction of a bacterial population in a physiological state that enables them to survive otherwise lethal doses of antibiotics. While these cells remain in the state of persistence, they cannot be killed by conventional antibiotics, unless the cells phenotypically switch to the normal cell state and become susceptible to antibiotics again [1]. Persisters are enriched in biofilms [2] and implicated in many chronic infections such as tuberculosis and relapse of infections such as recurrent urinary tract infection or cystic fibrosis [3–8]. Unlike antibiotic-resistant mutant cells, persisters are phenotypic variants that survive treatments without acquiring heritable genetic changes [9]. However, prolonged persistence creates favorable conditions for the emergence of the mutant cells [10,11].

Although the term *persister* was coined in the 1940s [12], our fundamental knowledge of persisters has accelerated only in the last two decades with the advent of new technologies enabling us to study cell heterogeneity [1,13]. Persisters survive via a plethora of putative molecular mechanisms [14], and recent studies have started shedding light on how diverse and multifaceted phenomena can link effects of initial states and environmental factors to phenotypic changes during persister formation, survival, and return to normal state [14–20]. In view of that complexity, developing anti-persister therapeutics remains a challenge. Such development can be broadly classified into two categories: (a) developing new anti-persister drugs, and the most common approach (b) manipulating the dosing regimen of approved antibiotics, used either individually or in combination. The former relies on detailed knowledge about persister mechanisms (formation, survival, and resuscitation) and is certainly significantly more time-consuming and resource-intensive than the latter. Within the latter category, strategies can be based on bacterial population dynamics without complete knowledge of molecular mechanisms, capitalizing instead on the back and forth switching of persisters from normal state to persistence and vice-versa. The idea of periodic pulse dosing to kill persisters is as old as the term persister itself [12]. Yet, there are only sporadic studies on pulse dosing, examining *in vitro* efficacy [21,22] and model fitting of experimental data or characterization of effective pulse dosing strategies [23–27]. A remaining challenge is a simple systematic design of an effective periodic pulse dosing regimen, comprising periods of antibiotic administration at high and low concentrations successively. Indeed, the alternating periods of antibiotic application (on) and removal (off) are critical to the success of pulse dosing strategies [22,28], as use of an inappropriate strategy fails to achieve eradication [29,30]. Attempts to connect experiments and modelling [28] have underscored the importance of characterizing optimal dosing regimens in a simple quantitative fashion.

The present study aims at addressing this issue. The specific contributions of this study are (a) rigorous theoretical justification that the efficacy of pulse dosing with alternating on/off periods of antibiotic administration depends on the ratio of the corresponding on/off periods of a pulse rather than on their individual values; (b) explicit formulas for robustly optimal values of this ratio in terms of easily estimated parameters; and (c) experimental confirmation *in vitro* of both positive and negative model predictions (bacterial eradication or not, respectively).

In the rest of the paper, we describe our experimental and modeling studies, present our main results, and close with suggestions for future studies. Proofs and details, to the extent that they provide insight, are included in appendices.

## 2 MATERIALS AND METHODS

### 2.1 Experimental

#### *2.1.1 Bacterial strain and plasmid*

*Escherichia coli* wild-type (WT) with a pQE-80L plasmid encoding a green fluorescent protein (GFP) was used. These were obtained from Dr. Mark P. Brynildsen of Princeton University.

#### *2.1.2 Media and chemicals*

Luria-Bertani (LB) broth was used for all liquid cultures. LB broth was prepared by dissolving its components (10g Tryptone, 10 g Sodium Chloride, 5 g Yeast Extract) in 1 L distilled water and sterilized with an autoclave. Ampicillin (Sigma Aldrich) was used to treat cells at a constant dose of 100 $\mu$g/mL. Phosphate Buffered Saline (PBS) was used to wash the cells to remove Ampicillin. LB agar medium was prepared by dissolving 40 g LB agar premix in 1 L DI water and sterilized with an autoclave. LB agar medium was used to enumerate colony forming units (CFUs) of *E. coli* [13,31,32].

#### *2.1.3 Constant (control) and pulse dosing experiments*

Bacteria were exposed to Ampicillin in two ways: at constant Ampicillin concentration (control) and at pulsed antibiotic concentration of the same amplitude (pulse on/off dosing, Fig 1).

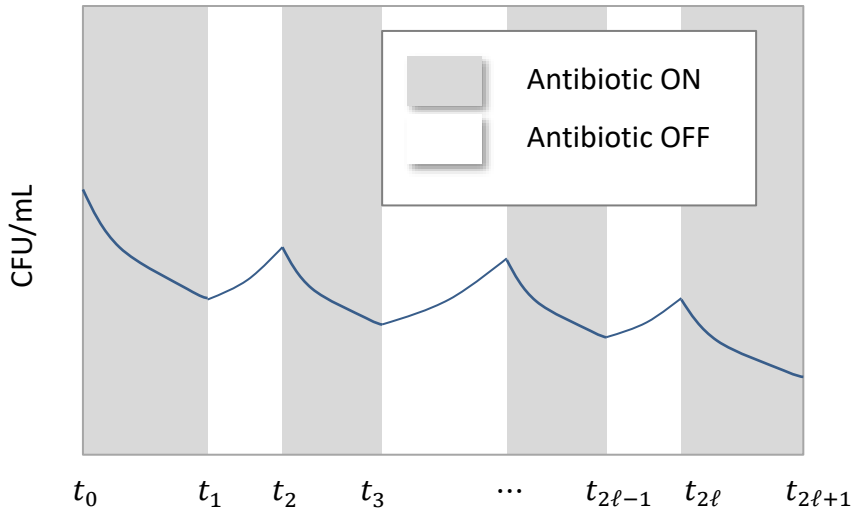


Fig 1. A schematic of the outcome of a pulse dosing regimen showing declining peaks and dips of a bacterial cell population over time.

Each pulse experiment was started by inoculating (1:100-fold) an overnight (24 h) culture of *E. coli* into 25 ml of LB. For selection and retention of plasmids in bacterial cells, 50 µg/mL

kanamycin was added in culture media [32]. To induce fluorescent protein expression, 1 mM IPTG was used [32]. The overnight culture was prepared from frozen glycerol stock (-80 ºC). All cells were cultured in a shaker at 37°C and 250 rpm. The pulse dosing schedule was: (a) expose bacteria to Ampicillin (100 $\mu$g/mL) for $t_{\text{on}}$ h, and (b) wash treated cells and grow in fresh media for $t_{\text{off}}$ h. Treated cells were washed with PBS buffer solution to remove the antibiotics. Cells were serially diluted in PBS using 96-well plates, spotted on LB agar, and incubated at 37 °C for 16 h to enumerate CFUs. Bacteria population size was assessed by colony counting on LB-Agar plates.

## 2.2 Modelling and Simulation

A two-state model [1], comprising two cell-balance differential equations for normal and persister cells, was used in all analysis:

$$\frac{dn}{dt} = K_n n(t) + bp(t) \tag{1}$$

$$\frac{dp}{dt} = an(t) + K_p p(t) \tag{2}$$

or, equivalently,

$$\underbrace{\begin{bmatrix} dn/dt \\ dp/dt \end{bmatrix}}_{d\mathbf{x}/dt} = \underbrace{\begin{bmatrix} K_n & b \\ a & K_p \end{bmatrix}}_{\mathbf{A}} \underbrace{\begin{bmatrix} n(t) \\ p(t) \end{bmatrix}}_{\mathbf{x}(t)} \tag{3}$$

where

$n(t) =$ Number of normal cells at time $t$

$p(t) =$ Number of persister cells at time $t$

$\mathbf{x}(t) \stackrel{\text{def}}{=} \begin{bmatrix} n(t) \\ p(t) \end{bmatrix}$

$\mathbf{A} \stackrel{\text{def}}{=} \begin{bmatrix} K_n & b \\ a & K_p \end{bmatrix}$

$a =$ switch rate from normal to persister state

$b =$ switch rate from persister to normal state

$K_n \stackrel{\text{def}}{=} \mu_n - k_n - a =$ net decline / growth rate of normal cells

$K_p \stackrel{\text{def}}{=} \mu_p - k_p - b =$ net decline / growth rate of persister cells

$\mu_n, \mu_p =$ growth rate of normal or persister cells, respectively

$k_n, k_p =$ kill rate of normal or persister cells, respectively

The parameters $a, b, K_n, K_p$ in eqns. (1) and (2) are generally distinct when the antibiotic is administered or not (on/off), resulting in corresponding matrices $\mathbf{A}_{\text{on}}, \mathbf{A}_{\text{off}}$ in eqn. (3). In the constant dosing (control) experiment the antibiotic remained always on, whereas for pulse dosing experiments the antibiotic alternated between on (administered) and off (not administered) with corresponding durations $t_{\text{on}}, t_{\text{off}}$. Therefore, to fit the full data set (at constant and pulse dosing) by eqns. (1) and (2), parameter estimation generally entailed eight values for estimates of

$\{a, b, K_n, K_p\}_{\text{off}}$ and $\{a, b, K_n, K_p\}_{\text{on}}$ during on and off periods, respectively. In addition, because data fit relied on measurements of the total number of cells,

$$c(t) \stackrel{\text{def}}{=} n(t) + p(t) \tag{4}$$

a ninth parameter, namely the initial fraction of persister cells, $f_0$, was estimated.

Mathematica and MATLAB were used for all modelling, parameter estimation, and analysis computations.

# 3 RESULTS

We present first a theoretical analysis for characterization of optimal pulse dosing regimens based on the model of eqns. (1) and (2), and subsequently present a series of experiments for validation of analysis results *in vitro*.

## 3.1 Design of pulse dosing for rapid bacterial population reduction

### *3.1.1 Characterizing $\{t_{\text{on}}, t_{\text{off}}\}$ for decline of a bacterial population*

Analysis of eqns. (1) and (2) (SI APPENDIX A) suggests that successive local peaks of the bacterial population size, $c(t)$, at times $t_{2\ell} \stackrel{\text{def}}{=} \ell(t_{\text{on}} + t_{\text{off}})$, as generally depicted in Fig 1, are characterized as

$$c(t_{2\ell}) = p_1\lambda_1^{\ell} + p_2\lambda_2^{\ell}, \ \ell = 0, 1, 2, \ldots \tag{5}$$

where $\lambda_1, \lambda_2$ are the eigenvalues of the matrix

$$\mathbf{M} \stackrel{\text{def}}{=} \exp(\mathbf{A}_{\text{off}} t_{\text{off}}) \exp(\mathbf{A}_{\text{on}} t_{\text{on}}) \tag{6}$$

and $p_1, p_2$ are coefficients depending on the model parameters and initial conditions.

It can be shown (SI APPENDIX A) that $\lambda_1, \lambda_2$ in eqn. (5) are inside the unit disk. As a result, the pattern of $c(t_{2n})$ in eqn. (5) is downward if and only if the respective on/off periods of pulse dosing, $t_{\text{on}}, t_{\text{off}}$, satisfy the inequality

$$\boxed{\frac{t_{\text{off}}}{t_{\text{on}}} < \left(\frac{t_{\text{off}}}{t_{\text{on}}}\right)_c \stackrel{\text{def}}{=} -\frac{K_{n,\text{on}}}{K_{n,\text{off}}}} \tag{7}$$

Note that the critical value $(t_{\text{off}}/t_{\text{on}})_c$ is positive, because $K_{n,\text{on}} < 0, K_{n,\text{off}} > 0$.

As an example, for the estimates $K_{n,\text{on}}, K_{n,\text{off}}$ shown in Table 1, eqn. (7) yields

$$\frac{t_{\text{off}}}{t_{\text{on}}} < 2.8 \tag{8}$$

for peak-to-peak decline, as shown in Fig 2.

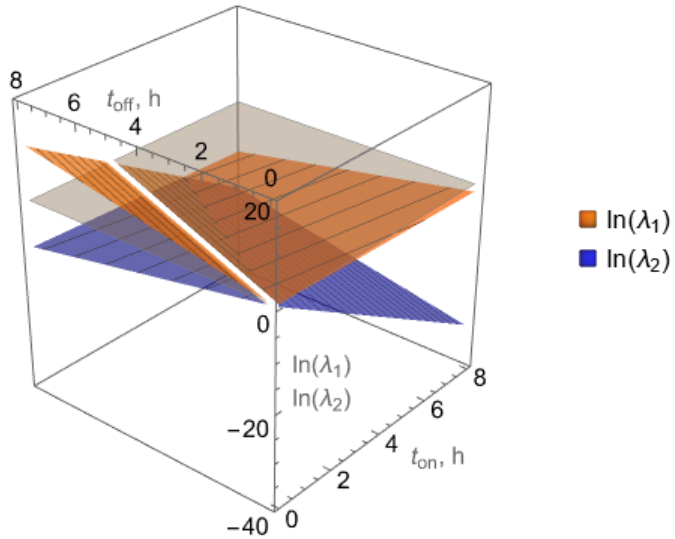


Fig 2. Eigenvalues $\lambda_1, \lambda_2$ of the matrix $\mathbf{M} \stackrel{\text{def}}{=} \exp(\mathbf{A}_{\text{off}} t_{\text{off}}) \exp(\mathbf{A}_{\text{on}} t_{\text{on}})$ governing successive peaks of the bacterial population size, $c(t_{2n})$, under pulse dosing with successive on/off pulses of respective durations $t_{\text{on}}, t_{\text{off}}$, given parameter values in Table 1. Values of $t_{\text{on}}, t_{\text{off}}$ that keep both $\lambda_1, \lambda_2$ below 1 (equivalently $\ln(\lambda_1)$, $\ln(\lambda_2)$ below 0) are shown. The white line corresponding to $(t_{\text{off}}/t_{\text{on}})_c \approx 2.8$, eqn. (8), on the gray plane at 0 indicates the threshold (critical) value of $t_{\text{off}}/t_{\text{on}}$, above which $\lambda_1 > 1$.

### *3.1.2 Characterizing $\{t_{\text{on}}, t_{\text{off}}\}$ for rapid peak-to-peak decline of the bacterial population*

For pulse dosing with fixed on/off periods $t_{\text{on}}, t_{\text{off}}$ that satisfy the inequality in eqn. (7), it can be shown (SI APPENDIX B) that eqn. (3) implies that successive peaks of $c(t)$ at times $t_{2n}$ (Fig 1) decline exponentially over time at a rate, $k$ characterized as

$$\boxed{k \stackrel{\text{def}}{=} \frac{\sqrt{\ln(\lambda_1)\ln(\lambda_2)}}{t_{\text{on}}+t_{\text{off}}} = \frac{\sqrt{(K_{n,\text{off}}x+K_{n,\text{on}})(K_{p,\text{off}}x+K_{p,\text{on}})}}{1+x}} \tag{9}$$

where

$$x \stackrel{\text{def}}{=} \frac{t_{\text{off}}}{t_{\text{on}}} \tag{10}$$

or, equivalently, with a time constant, $\tau = 1/k$.

It follows immediately (SI APPENDIX A) that the maximum peak-to-peak decline rate for $k$ (as shown in eqn. (9)) is attained at

$$\boxed{\left(\frac{t_{\text{off}}}{t_{\text{on}}}\right)_{\text{opt}} = \frac{2R_nR_p-R_n-R_p}{2-R_n-R_p} \approx \frac{R_n}{R_n-2}} \tag{11}$$

where

$$R_p \stackrel{\text{def}}{=} \frac{K_{p,\text{on}}}{K_{p,\text{off}}}, \quad R_n \stackrel{\text{def}}{=} \frac{K_{n,\text{on}}}{K_{n,\text{off}}} \tag{12}$$

and the approximation in eqn. (11) is based on

$$\frac{K_{p,\text{on}}}{K_{p,\text{off}}} \approx 0 \tag{13}$$

Note that $(t_{\text{off}}/t_{\text{on}})_{\text{opt}}$ in eqn. (11) depends on the ratios $R_p \stackrel{\text{def}}{=} K_{p,\text{on}}/K_{p,\text{off}}$, $R_n \stackrel{\text{def}}{=} K_{n,\text{on}}/K_{n,\text{off}}$, rather than on the individual values of $K_{p,\text{on}}, K_{p,\text{off}}, K_{n,\text{on}}, K_{n,\text{off}}$. Note also that combination of eqns. (11) and (7) immediately connects the optimal and critical values of the ratio $t_{\text{off}}/t_{\text{on}}$ as

$$\left(\frac{t_{\text{off}}}{t_{\text{on}}}\right)_{\text{opt}} \approx \frac{(t_{\text{off}}/t_{\text{on}})_c}{(t_{\text{off}}/t_{\text{on}})_c+2} \tag{14}$$

Application of eqn. (11) yields a profile or the optimal ratio $(t_{\text{off}}/t_{\text{on}})_{\text{opt}}$ in terms of the ratios $R_p, R_n$ in eqn. (12) as shown in Fig 3. In that figure, estimates from the experimental data of Fig 2 fitted by parameter estimates in Table 1 are used to mark the indicated point.

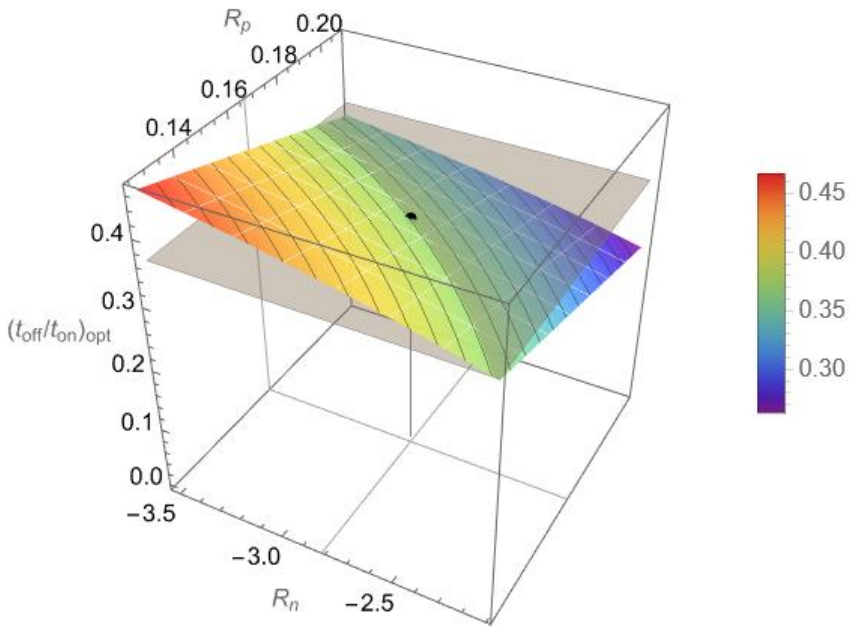


Fig 3. Optimal values $(t_{\text{on}}/t_{\text{off}})_{\text{opt}}$ of the ratio $t_{\text{on}}/t_{\text{off}}$ that yield maximum decline rate, $k$, of successive peaks of bacterial population counts, $c(t_{2\ell})$, as a function of the quantities $R_p \stackrel{\text{def}}{=} \frac{K_{p,\text{on}}}{K_{p,\text{off}}}$, $R_n \stackrel{\text{def}}{=} \frac{K_{n,\text{on}}}{K_{n,\text{off}}}$, according to eqn. (11). Values of $R_n$, $R_p$ are considered in the range $\pm 25\%$ of the experimentally estimated values, which correspond to $(t_{\text{on}}/t_{\text{off}})_{\text{opt}} \approx 0.4$, marked by the black dot and gray horizontal plane through it.

To visualize eqns. (7), (9), and (11), estimates of $\{K_n, K_p\}_{\text{off}}$ and $\{K_n, K_p\}_{\text{on}}$ in Table 1 were used to produce a characterization of the peak-to-peak decline rate as a function of $t_{\text{on}}, t_{\text{off}}$, as shown in Fig 4.

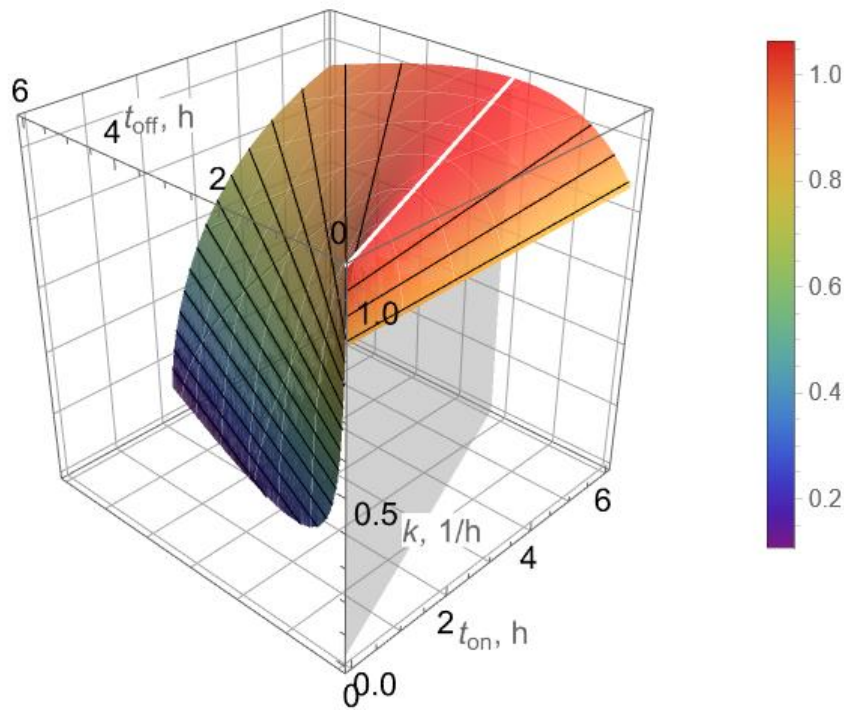


Fig 4. Peak-to-peak decline rate, $k$, for bacterial count peaks $c(t_{2\ell})$ (eqn. (9)) as a function of on/off pulse durations, $t_{\text{on}}, t_{\text{off}}$, respectively, for pulse dosing. The decline rate, $k$, achieves a maximum for $(t_{\text{off}}/t_{\text{on}})_{\text{opt}} \approx 0.4$ according to eqn. (11) (white line) and remains relatively flat for small variations of $t_{\text{on}}, t_{\text{off}}$ near $(t_{\text{off}}/t_{\text{on}})_{\text{opt}} \approx 0.4$. Note also that isolines (black) are straight, indicating dependence of $k$ on $(t_{\text{off}}/t_{\text{on}})$ rather than on individual values of $t_{\text{on}}, t_{\text{off}}$.

A remarkable implication of eqn. (11) is that an optimal ratio $t_{\text{off}}/t_{\text{on}}$ (in the sense defined in this section) can be approximately assessed by mere knowledge of the ratio $K_{n,\text{on}}/K_{n,\text{off}}$, which, in turn, can be easily obtained from two simple short-term experiments, namely standard time-growth and time-kill. The corresponding initial slopes in such experiments immediately yield $K_{n,\text{off}}$ (time-growth) and $K_{n,\text{on}}$ (time-kill), as discussed next. This is a significant simplification of the parameter estimation task for the purpose of pulse dosing regimen design, because it reduces the number of parameters to be estimated from nine (cf. section 2.2) to two. In addition, these two parameters are much easier to estimate than the remaining seven, whose accurate estimates are hard to obtain, as discussed in section 3.3.

### 3.2 Constant and pulse dosing experiments

Data from a simple time-growth experiment (no antibiotic) and a time-kill experiment (Ampicillin at constant concentration 100 μg/mL) are shown in Fig 5. The slopes from respective curve fits of the data in Fig 5 yield

$$K_{n,\text{off}}/\ln(10) \approx 0.5,\ K_{n,\text{on}}/\ln(10) = -1.4 \tag{15}$$

Detailed statistics are provided in SI APPENDIX C. Note that the pattern shown in Fig 5(b) indicates exponential decline (corresponding to a straight line of the bacterial population logarithm) as the almost horizontal part of the biphasic trend, which is typical of persisters [2], has not yet been reached within 3 hours. That trend is reached through continuation of the experiment after 3 hours, as indicated by the red data points and corresponding bend of the line fitted in Fig 6.

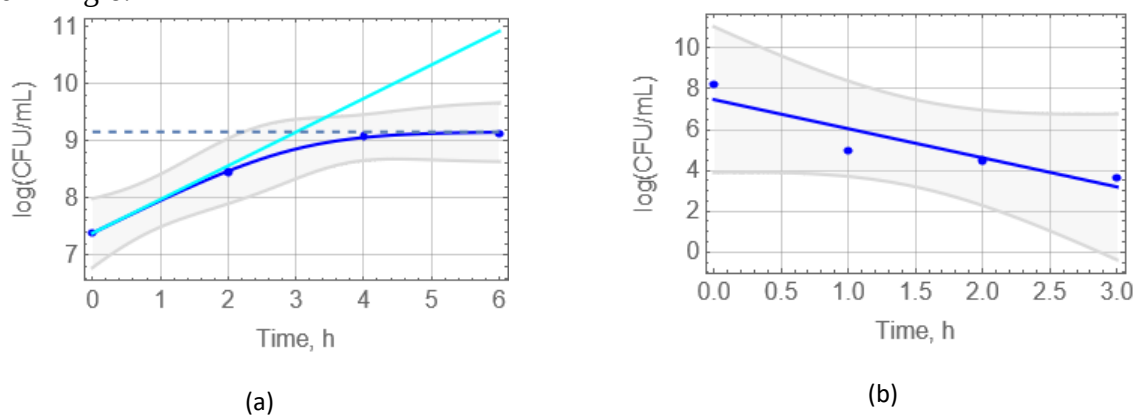


Fig 5. Time-growth (a) and time-kill (Ampicillin at 100 μg/mL) (b) experiments for generation of data to assess $t_{\text{on}}/t_{\text{off}}$ for design of pulse dosing. 95%-confidence bands are shown. The slope of the cyan straight line (a) indicates the initial slope of the blue line and corresponds to $K_{n,\text{off}}/\ln(10)$, whereas the blue line slope (b) is $K_{n,\text{on}}/\ln(10)$.

Using the above two estimates for $K_{n,\text{off}}, K_{n,\text{on}}$ in eqn. (12) to calculate $R_n$ and substituting the resulting value of $R_n$ into eqn. (11) yields

$$\left(\frac{t_{\text{off}}}{t_{\text{on}}}\right)_{\text{opt}} \approx 0.6 \tag{16}$$

Therefore, to be close to the value of 0.6, pulse dosing with

$$t_{\text{on}} = 3\text{h}, t_{\text{off}} = 2\text{h} \tag{17}$$

was implemented in validation experiments *in vitro*.

The outcome of pulse dosing using the above $t_{\text{on}}, t_{\text{off}}$, along with additional data for continuation of the constant dosing (control) experiment to 13h, are shown in Fig 6. In the case of constant dosing, colonies were seen in all replicates at the end of the 13h treatment $(5 - 100\ \text{CFU/mL})$ whereas in the case of pulse dosing no colony was observed in any replicate in the latter part of the last $t_{\text{on}}$ cycle. Note that both Fig 5 and Fig 6 indicate a 5 log decrease of viable cells over the first 3 hours.

### 3.3 Model parameter estimation with full data set

To confirm that the model used in the analysis for development of the formulas applied in the approach proposed to pulse dosing design, the parameters in eqns. (1) and (2) were fit to the full

set of experimental data of Fig 6, with corresponding curves shown in Fig 6 and parameter estimates shown in Table 1.

Table 1 Parameter estimates fitting the experimental data of Fig 6. (standard errors reported)

| Parameter | **Antibiotic on** | **Antibiotic off** |
|---|---|---|
| $K_n$ | $-3.8 \pm 0.4$ | $1.35 \pm 0.09$ |
| $K_p$ | $-0.2 \pm 0.2$ | $-1.2 \pm 0.4$ |
| $a$ | 0 | 0 |
| $b$ | 0 | $1.2 \pm 0.4$ |
| $f_0$ | $9\mathrm{E}-07 \pm 1.6\mathrm{E}-05$ | |
| $\log_{10} c_0$ | $7.8 \pm 0.4$ | |

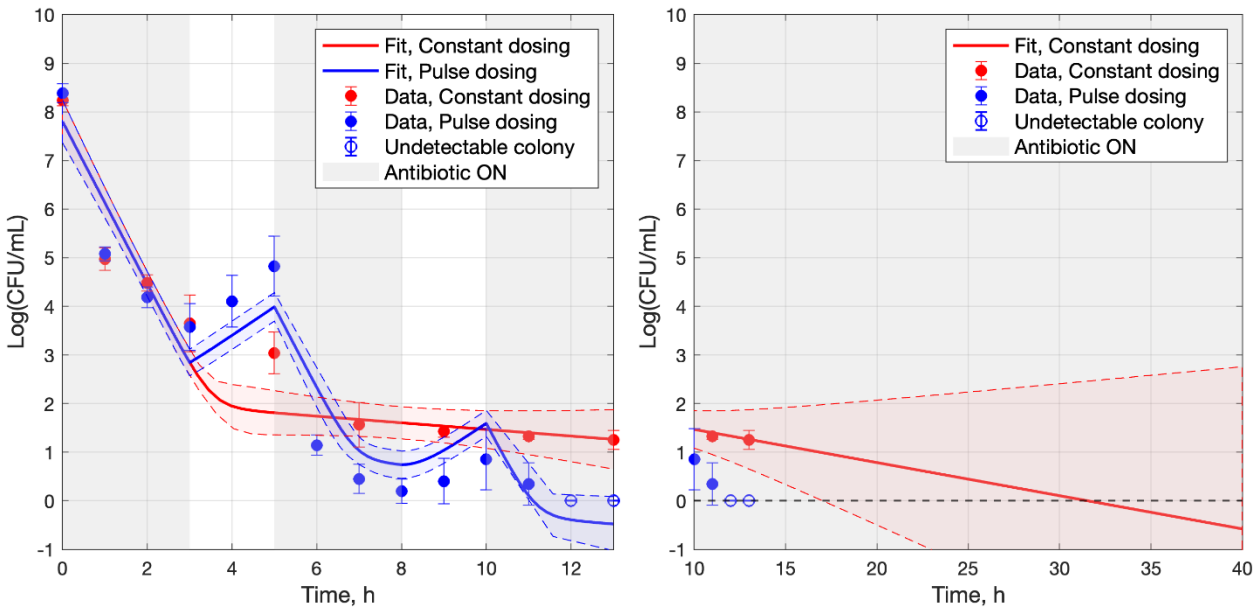


(a) (b)

Fig 6. (a) Experimental data and model fit for bacterial population over time, resulting from constant dosing (red) and uniform pulse dosing at ratio $t_{\mathrm{off}}/t_{\mathrm{on}} = 2/3$ (blue). The hollow blue circles at 12h and 13h are set to 0 by convention, to indicate undetectable colony forming units (CFU). (b) Fitted model projection for the outcome of constant dosing to reach 0. 68%-confidence bands (1 standard error) are shown.

### 3.4 Pulse dosing design validation

Eqns. (7) and (8) indicate that bacteria eradication would be achieved if the pulse dosing period ratio $t_{\mathrm{off}}/t_{\mathrm{on}}$ remained below 2.8, based on the short-term data fit (Fig 5), or below 2.4, based on full data fit (Fig 6). This assessment is confirmed via both simulation and experiment.

### *3.4.1 Simulation*

Integration of eqns. (1) and (2) for parameter estimates based on Fig 6 yields the results of Fig 7. That figure shows profiles of the total bacterial population over time for various values of $\{t_{\text{on}}, t_{\text{off}}\}$, anticipated by Fig 4 to correspond to either eradication or growth of the population.

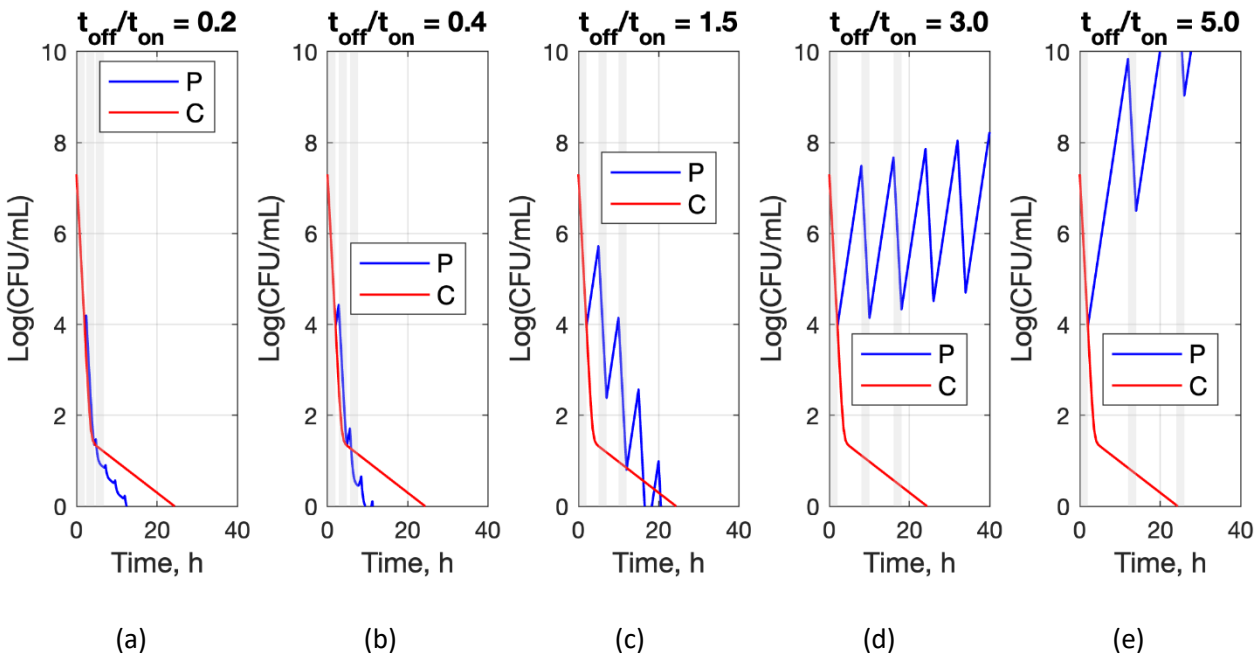


Fig 7. Solution of eqns. (1) and (2) for constant dosing (red) and for uniform pulse dosing (blue) with $t_{\text{on}} = 2\text{h}$ and different values of $t_{\text{off}}/t_{\text{on}}$, given estimates of $\{a, b, K_n, K_p\}_{\text{off}}$ and $\{a, b, K_n, K_p\}_{\text{on}}$ obtained from the experimental data of Fig 6. Outcomes are as anticipated by Fig 4, i.e. eradication at different rates is observed in (a)-(c) and lack of eradication in (d), (e).

### *3.4.2 Experiment*

In addition to the experimental data in Fig 6, which confirmed rapid bacterial eradication for pulse dosing at ratio $t_{\text{off}}/t_{\text{on}} = 2/3$, example cases of pulse dosing at ratios $t_{\text{off}}/t_{\text{on}}$ anticipated by the developed theory and by computer simulations not to result in bacterial eradication were also tested through *in vitro* experiments, as shown in Fig 8. This figure shows the outcome (dots) of two pulse dosing experiments corresponding to the same $t_{\text{off}}/t_{\text{on}} = 6$, above the critical value $(t_{\text{off}}/t_{\text{on}})_c = 2.8$ (eqn. (8)), for $t_{\text{on}} = 0.5\text{h}$ and $t_{\text{on}} = 3\text{h}$. Model predictions (eqns. (1) and (2) with parameter estimates from Table 1 based on data of Fig 6) are also shown.

Note that for $\{t_{\text{on}}, t_{\text{off}}\} = \{3\text{h}, 18\text{h}\}$ the linear model of eqns. (1) and (2) correctly predicts the observed peak-to-peak upward trend, but the model crosses the bacterial population saturation limits (eqn. (SI-23)) which are at about 9 $\log(\text{CFU/mL})$ (SI APPENDIX C) hence the quantitative discrepancy.

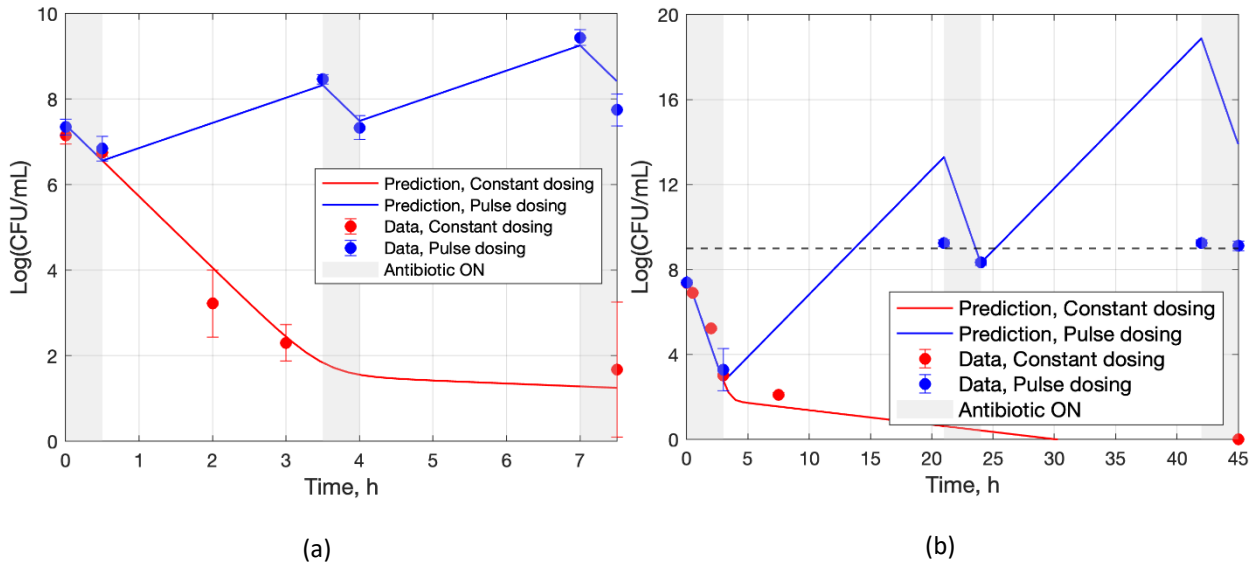


Fig 8. Experimental values (dots) and model predictions (lines) for constant dosing (red) and pulse dosing with $t_{\mathrm{off}}/t_{\mathrm{on}} = 6 > (t_{\mathrm{off}}/t_{\mathrm{on}})_c$ (blue) for (a) $\{t_{\mathrm{on}}, t_{\mathrm{off}}\} = \{0.5\mathrm{h}, 3\mathrm{h}\}$ and (b) $\{t_{\mathrm{on}}, t_{\mathrm{off}}\} = \{3\mathrm{h}, 18\mathrm{h}\}$.

Additional experiments were also conducted to test the robustness of pulse dosing in case of non-uniform perturbations of $t_{\mathrm{on}}$ around 3h and $t_{\mathrm{off}}$ around 2h. The results, shown in Fig 9, suggest rapid bacterial eradication (within about 10h), on par with uniform pulse dosing (cf. results shown in Fig 6 and Fig 7).

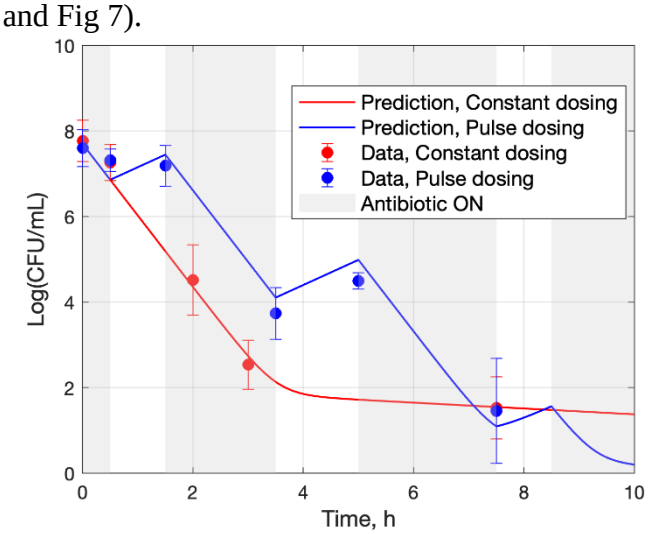


Fig 9. Outcome of non-uniform pulse dosing (and control) for non-uniform perturbations of pulse durations around their nominal values $t_{\mathrm{on}} = 3\mathrm{h}, t_{\mathrm{off}} = 2\mathrm{h}$.

# 4 Discussion

## 4.1 Summary of results

In summary, the presented method to pulse dosing regimen design relies on eqn. (11), which expresses the optimal ratio $(t_{\mathrm{off}}/t_{\mathrm{on}})_{\mathrm{opt}}$ as approximately a function of $R_n \stackrel{\mathrm{def}}{=} K_{n,\mathrm{on}}/K_{n,\mathrm{off}}$, where

the parameters $K_{n,\text{off}}, K_{n,\text{on}}$ are easy to obtain from the early parts of time-growth and time-kill experiments, respectively, as demonstrated in Fig 5. Starting with this, the efficacy of a near optimal proposed design is experimentally validated in Fig 6, the sub-optimality of designs with $t_{\text{off}}/t_{\text{on}}$ other than $(t_{\text{off}}/t_{\text{on}})_{\text{opt}}$ is illustrated in Fig 7, predictions for the complete failure of pulse dosing regimens with $t_{\text{off}}/t_{\text{on}}$ above the critical value (eqn. (7)) are experimentally validated in Fig 8, and the robustness of proposed dosing regimen designs is experimentally validated in Fig 9.

Additional details are discussed in sections 4.2 and 4.3. Finally, an elucidation of literature results in view of the proposed theory is presented in section 4.4.

## 4.2 Design of pulse dosing for rapid bacterial population reduction

### *4.2.1 Characterizing $\{t_{\text{on}}, t_{\text{off}}\}$ for decline of a bacterial population*

The analysis presented relies on the linear model of eqns. (1) and (2). That model is clearly not valid when the bacterial population reaches its saturation limits after long growth periods (e.g. Fig 5 (a) and eqn. (SI-23) in SI APPENDIX C). Therefore, eqn. (7), which places an upper bound on the ratio $t_{\text{on}}/t_{\text{off}}$ of pulse dosing, is understood to hold for values of $t_{\text{off}}$ that do not drive the bacterial population beyond logarithmic growth to saturation.

### *4.2.2 Characterizing $\{t_{\text{on}}, t_{\text{off}}\}$ for rapid peak-to-peak decline of the bacterial population*

Selection of the geometric average of two decline rate constants,

$$k_1 \stackrel{\text{def}}{=} -\frac{\ln(\lambda_1)}{(t_{\text{on}}+t_{\text{off}})},\ k_2 \stackrel{\text{def}}{=} -\frac{\ln(\lambda_2)}{(t_{\text{on}}+t_{\text{off}})} \tag{18}$$

in eqn. (9), captures well an overall decline rate (Fig 10) when early parts of the decline are important.

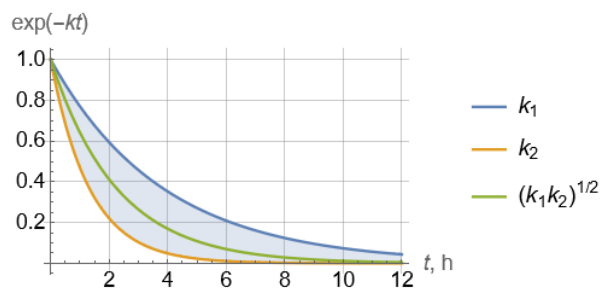


Fig 10. Exponential peak-to-peak decline rate modes corresponding to each individual rate $k_1, k_2$ (eqn. (18)) and the geometric average rate $k \stackrel{\text{def}}{=} (k_1 k_2)^{1/2}$ (eqn. (9)).

An alternative, focusing more on the long-term decline rate, would be to choose the dominant (smaller) of the two decline rates $k_1, k_2$ (Fig 10). The results would be somewhat different quantitatively, but of similar nature. This is exemplified in Fig 11, which is the counterpart of Fig 4. Simulations shown in Fig 7 clearly indicate that predictions of peak-to-peak decline rates made by Fig 4 are quantitatively more reliable than those made by Fig 11.

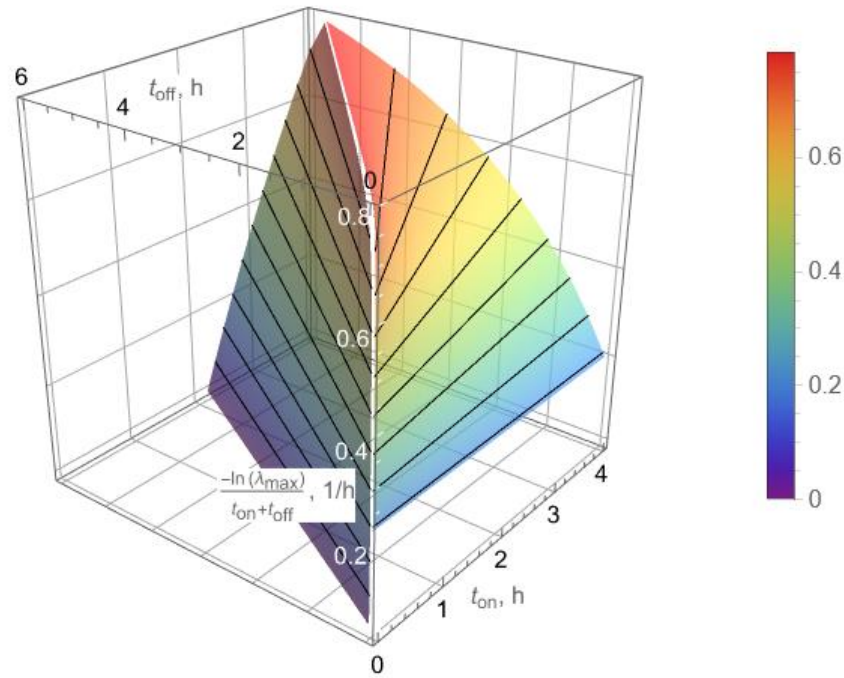


Fig 11. Peak-to-peak actual-time decline rate corresponding to the larger (slower) of the two eigenvalues $\lambda_1, \lambda_2$ of the matrix $\mathbf{M}$ as a function of $t_{\text{on}}, t_{\text{off}}$ for the values of $K_{n,\text{on}}$, $K_{p,\text{on}}$, $K_{n,\text{off}}$, $K_{p,\text{off}}$ in Table 1. The crease line (white), where the two surfaces intersect, corresponds to eqn. (SI-16) and characterizes the highest peak-to-peak actual-time decline rate, for $t_{\text{off}}/t_{\text{on}} = 1.5$.

The quantitative analysis presented in section 3.1 focuses on the rate of peak-to-peak decline, with the intent to design pulse dosing regimens for rapid bacterial eradication. A somewhat more accurate characterization of time to eradication would be provided by focusing on the rate of dip-to-dip decline (c.f. Fig 6 and Fig 7). It can be shown (eqns. (SI-1) and (SI-2) in SI APPENDIX A), however, that both peaks and dips of the bacterial population follow the same rate, governed by the eigenvalues $\lambda_1, \lambda_2$ of the matrix $\mathbf{M}$ (eqn. (6)). Because tracking peaks is simpler to analyze than tracking dips, the choice was made to focus on the former, leaving the latter for a future study.

In addition to the quantitative analysis that resulted in the selected values $t_{\text{on}} = 3\text{h}, t_{\text{off}} = 2\text{h}$ (eqn. (17)) for the pulse dosing experiment, heuristic analysis was also used to corroborate that choice, as follows:

In the early part of the constant dosing (control) experiment, it is evident (Fig 6) that around 3h persisters start becoming an increasingly significant fraction of the bacterial population (as manifest by the bend in the declining population logarithmic size) and subsequently dominate the population. Therefore, keeping the antibiotic on beyond 3h would

result in reduced killing rate. Furthermore, while turning the antibiotic off starts driving persisters back to normal cells, keeping it off beyond 2h would reach the limits of that drive. While the above analysis suggests that the selected of $t_{\text{on}}, t_{\text{off}}$ values are sensible, it cannot provide a general characterization of optimal values or establish the importance of the ratio $t_{\text{on}}/t_{\text{off}}$.

Related experiments [33] have found that persisters treated for 3h with Ampicillin were able to resuscitate after growth in fresh media for as little as 1h. In our experiments also, a manifold increase in kill rates when treated again with Ampicillin suggested that persisters resuscitated to normal cells indeed within an hour of growth in fresh media.

### 4.3 Modeling and parameter estimation

Estimation of the four model parameters in eqns. (1) and (2) faces the challenge that measurements of bacterial population size, eqn. (4), are linear combinations of the two solution modes, $q_1 \exp(\rho_1 t) + q_2 \exp(\rho_2 t)$ (SI APPENDIX D) with

$$\rho_{1,2} = \frac{1}{2}\left(K_n + K_p \pm \sqrt{4ab + (K_n - K_p)^2}\right) \tag{19}$$

which makes it difficult to estimate all four $\{K_n, K_p, a, b\}$ with good accuracy from data. Nevertheless, assumptions based on fundamental knowledge can facilitate estimation. These assumptions are in accordance with relevant literature [9] and similar observations in our own experiments.

When the antibiotic is on, it follows that $b \approx 0$, because persisters remain dormant, and $a \gtrsim 0$, as some normal cells switch to persisters due to antibiotic stress. Estimation of a nonzero $a$ yielded a very small value, in agreement with the assumption $a \approx 0$, i.e. that persisters can be sourced to the initial pool of cells.

When there is no antibiotic and cells are grown in fresh media, it follows that $a \approx 0$, as the tendency of normal cells to become dormant is negligible during the early exponential phase (e.g. in less than 3h of growth), whereas $b > 0$, as persisters will be resuscitated shortly (e.g. within an hour) after inoculation in fresh media [13,33,34]. In addition, $K_{p,\text{on}} \approx -b$, because $\mu_{p,\text{on}} \approx 0$ and $k_{p,\text{on}} \approx 0$.

The different bactericidal outcomes produced by constant and pulse dosing are evident in Fig 6(a), where the (one-standard-error) confidence bands towards the end of the experimental period of 13h are clearly separated, with pulse dosing yielding no detectable bacterial load and constant dosing leaving a load of about $20\log(\text{CFU/mL})$ at 13h. In addition, Fig 6(b) shows the fitted model projection until the bacterial population outcome resulting from constant dosing reaches 0 at about 30h, long after pulse dosing has reached the same outcome in less than 12h.

### 4.4 Application of the proposed theory to literature data

To further test the ability of the proposed theory to predict the bactericidal efficacy of pulse dosing regimens, we analyzed experimental data from two studies in literature [28][29]. These studies presented pulse dosing regimens on bacterial populations with persister bacteria.

To perform the test, estimates of $K_{n,\mathrm{on}}$ (decline slope of the logarithmic population of *normal* cells under antibiotic exposure) were obtained from data presented in corresponding figures for both studies (Table 2 and Table 3); and estimates of $K_{n,\mathrm{off}}$ (growth slope of the logarithmic population of *normal* cells in growth) for [29] were either obtained from a corresponding figure in [28] (Table 2) or estimated based on past experience (Table 3). The critical values of the ratio $t_{\mathrm{off}}/t_{\mathrm{on}}$ were subsequently calculated for both references from eqns. (7) and (11), respectively (Table 2 and Table 3). These values were then compared to the actual values used in experiments presented in each reference cited. Corresponding predictions from this comparison ere consistent with data in all cases. Specifically, Table 2 indicates that bacterial populations declined when $t_{\mathrm{off}}/t_{\mathrm{on}} < (t_{\mathrm{off}}/t_{\mathrm{on}})_c$ (eqn. (7)) and grew when $t_{\mathrm{off}}/t_{\mathrm{on}} > (t_{\mathrm{off}}/t_{\mathrm{on}})_c$. In fact, the peak-to-peak slopes shown in Figure 4 of [28] are in agreement with the discrepancy between the values of $t_{\mathrm{off}}/t_{\mathrm{on}}$ used and the critical or optimal values. Similarly, Table 3 indicates that $t_{\mathrm{off}}/t_{\mathrm{on}}$ in [29] is higher than the critical value $(t_{\mathrm{off}}/t_{\mathrm{on}})_c$ for all four strains focused on, in agreement with observed increasing persister percentages in the bacterial populations studied.

For completeness, the optimal ratios $(t_{\mathrm{off}}/t_{\mathrm{on}})_{\mathrm{opt}}$ are also shown in Table 2 and Table 3.

Table 2. Literature data analysis to test proposed theory for pulse dosing regimen design

| Data source | [28] | | |
|---|---|---|---|
| Bacteria Strain | *S. aureus* | | |
| Antibiotic | Ofloxacin | | |
| $K_{n,\mathrm{on}}$ $(\mathrm{h}^{-1})$ | $-0.6$ (Figure 4c) | | |
| $K_{n,\mathrm{off}}$ $(\mathrm{h}^{-1})$ | 2.5 (Figure 4a) | | |
| $\left(\frac{t_{\mathrm{off}}}{t_{\mathrm{on}}}\right)_c = -\frac{K_{n,\mathrm{on}}}{K_{n,\mathrm{off}}}$ (eqn. (7)) | 0.24 | | |
| $\frac{t_{\mathrm{off}}}{t_{\mathrm{on}}}$ used in [28] | 4h/20h $= 0.2$ | 9h/15h $= 0.6$ | 16h/8h $= 2$ |
| $\frac{t_{\mathrm{off}}}{t_{\mathrm{on}}}$ used in [28] $< \left(\frac{t_{\mathrm{off}}}{t_{\mathrm{on}}}\right)_c$ ? (eqn. (7)) | Yes | No | No |
| Bacterial population decline? | Yes ([28] Figure 4b) | No ([28] Figure 4c) | No ([28] Figure 4d) |
| $\left(\frac{t_{\mathrm{off}}}{t_{\mathrm{on}}}\right)_{\mathrm{opt}} \approx \frac{\left(\frac{t_{\mathrm{off}}}{t_{\mathrm{on}}}\right)_c}{\left(\frac{t_{\mathrm{off}}}{t_{\mathrm{on}}}\right)_c + 2}$ (eqns. (11), (14)) | 0.1 | | |

Table 3. Literature data analysis to test proposed theory for pulse dosing regimen design

| Data source | [29] | | | |
|---|---|---|---|---|
| Bacteria Strain | *P. aeruginosa* | *A. baumannii* | *K. pneumoniae* | *E. aerogenes* |
| Antibiotic | Amikacin | | | |
| $K_{n,\mathrm{on}}$ $(\mathrm{h}^{-1})$ | $-3$ ([29] FIG 2A) | $-3$ ([29] FIG 2A) | $-5$ ([29] FIG 2A) | $-5$ ([29] FIG 2A) |
| $K_{n,\mathrm{off}}$ $(\mathrm{h}^{-1})$ | 1 to 3 (Estimate) | 1 to 3 (Estimate) | 1 to 3 (Estimate) | 1 to 3 (Estimate) |
| $\left(\frac{t_{\mathrm{off}}}{t_{\mathrm{on}}}\right)_c = -\frac{K_{n,\mathrm{on}}}{K_{n,\mathrm{off}}}$ (eqn. (7)) | 1 to 3 | 1 to 3 | 1.7 to 5 | 1.7 to 5 |
| $\frac{t_{\mathrm{off}}}{t_{\mathrm{on}}}$ used in [29] | 43h/5h = 8.6 | 43h/5h = 8.6 | 43h/5h = 8.6 | 19h/5h = 3.8 |
| $\frac{t_{\mathrm{off}}}{t_{\mathrm{on}}}$ used in [29] $< \left(\frac{t_{\mathrm{off}}}{t_{\mathrm{on}}}\right)_c$ ? | No | No | No | No |
| Persister percentage decline? | No ([29] FIG 3a) | No ([29] FIG 3a) | No ([29] FIG 3a) | No ([29] FIG 3a) |
| $\left(\frac{t_{\mathrm{off}}}{t_{\mathrm{on}}}\right)_{\mathrm{opt}} \approx \frac{\left(\frac{t_{\mathrm{off}}}{t_{\mathrm{on}}}\right)_c}{\left(\frac{t_{\mathrm{off}}}{t_{\mathrm{on}}}\right)_c + 2}$ (eqn. (14)) | 0.3 to 0.6 | 0.3 to 0.6 | 0.5 to 0.7 | 0.5 to 0.7 |

## 1 CONCLUSIONS AND FUTURE WORK

We have developed a methodology for systematic design of pulse dosing regimens that can eradicate persistent bacteria. The methodology relies on explicit formulas that make use of easily obtainable data from time-growth and time-kill experiments with a bacterial population exposed to antibiotics. Several extensions of this work can be pursued, including:

- Test the outlined strategy on various pairs of pathogenic bacterial strains and antibiotics, including combinations of antibiotics for stubborn infections.
- Extend and test the developed methodology, both theoretically and experimentally, to
    - Clinically relevant pharmacokinetic profiles of antibiotic administration, e.g. periodic injection followed by exponential [35].
    - Reduced antibiotics concentration in consecutive cycles [36].
    - Ultimately in vivo studies
- The experiments presented used Ampicillin (a $\beta$-lactam antibiotic) which is a time-dependent antibiotic, namely it exhibits best efficacy if administered in periodic injections of as high concentration as possible. It is worth exploring the performance of the proposed pulse dosing design methodology to concentration-dependent antibiotics such as aminoglycosides and quinolones[37].

- Models developed using data from flow cytometry experiments [38] can better monitor the heterogeneity of a bacterial population, with potential improvements in modeling and, as a result, pulse dosing design.
- Extension to viable but not culturable cells: In addition to persisters, a well known bacterial phenotype that can survive exposure to antibiotics is viable but not culturable (VBNC) cells [39–41] . The pulse dosing methodology presented here can, in principle, be applied to such cells, as they can be restored to normal growth and susceptibility to antibiotics upon provision of appropriate stimuli [42,43]. However, experimentally studying this case poses different challenges, as standard cell cultures cannot be routinely used, and this is left for future exploration.

## 5 *ACKNOWLEDGEMENTS*

Michael Nikolaou and Garima Singh gratefully acknowledge substantial help provided by Sayed Golam Mohiuddin to set up and conduct the experimental part of the study.

## 6 REFERENCES

1. Balaban NQ, Merrin J, Chait R, Kowalik L, Leibler S. Bacterial persistence as a phenotypic switch. Science (1979). 2004;305: 1622–1625. doi:10.1126/science.1099390
2. Lewis K. Persister cells, dormancy and infectious disease. Nat Rev Microbiol. 2007;5: 48–56. doi:10.1038/nrmicro1557
3. Meylan S, Andrews IW, Collins JJ. Targeting Antibiotic Tolerance, Pathogen by Pathogen. Cell. 2018. doi:10.1016/j.cell.2018.01.037
4. Torrey HL, Keren I, Via LE, Lee JS, Lewis K. High persister mutants in mycobacterium tuberculosis. PLoS One. 2016;11: 1–28. doi:10.1371/journal.pone.0155127
5. Zhang Y, Yew WW, Barer MR. Targeting Persisters for Tuberculosis Control. Antimicrob Agents Chemother. 2012;56: 2223 LP – 2230. doi:10.1128/AAC.06288-11
6. Keren I, Minami S, Rubin E, Lewis K. Characterization and Transcriptome Analysis of Mycobacterium tuberculosis Persisters. 2011 [cited 29 Oct 2019]. doi:10.1128/mBio.00100-11
7. Blango MG, Mulvey MA. Persistence of uropathogenic Escherichia coli in the face of multiple antibiotics. Antimicrob Agents Chemother. 2010;54: 1855–1863. doi:10.1128/AAC.00014-10
8. Mulvey MA, Schilling JD, Hultgren SJ. Establishment of a persistent Escherichia coli reservoir during the acute phase of a bladder infection. Infect Immun. 2001;69: 4572–4579. doi:10.1128/IAI.69.7.4572-4579.2001
9. Balaban NQ, Helaine S, Lewis K, Ackermann M, Aldridge B, Andersson DI, et al. Definitions and guidelines for research on antibiotic persistence. Nat Rev Microbiol. 2019;17: 441–448. doi:10.1038/s41579-019-0196-3
10. Windels EM, Michiels JE, Fauvart M, Wenseleers T, van den Bergh B, Michiels J. Bacterial persistence promotes the evolution of antibiotic resistance by increasing survival and mutation rates. ISME J. 2019;13: 1239–1251. doi:10.1038/s41396-019-0344-9

11. Levin-Reisman I, Ronin I, Gefen O, Braniss I, Shoresh N, Balaban NQ. Antibiotic tolerance facilitates the evolution of resistance. Science (1979). 2017;355: 826–830. doi:10.1126/science.aaj2191
12. Bigger JW. Treatment of Staphylococcal Infections With Penicillin By Intermittent Sterilisation. The Lancet. 1944;244: 497–500. doi:10.1016/S0140-6736(00)74210-3
13. Keren I, Kaldalu N, Spoering A, Wang Y, Lewis K. Persister cells and tolerance to antimicrobials. FEMS Microbiol Lett. 2004;230: 13–18. doi:10.1016/S0378-1097(03)00856-5
14. Goode O, Smith A, Zarkan A, Cama J, Invergo BM, Belgami D, et al. Persister Escherichia coli Cells Have a Lower Intracellular pH than Susceptible Cells but Maintain Their pH in Response to Antibiotic Treatment. 2021. doi:10.1128/mBio
15. Balaban NQ, Gerdes K, Lewis K, McKinney JD. A problem of persistence: Still more questions than answers? Nature Reviews Microbiology. 2013. pp. 587–591. doi:10.1038/nrmicro3076
16. Lewis K. Persister cells and infectious disease. Persister Cells and Infectious Disease. Springer International Publishing; 2019. doi:10.1007/978-3-030-25241-0
17. van den Bergh B, Schramke H, Michiels JE, Kimkes TEP, Radzikowski JL, Schimpf J, et al. Mutations in respiratory complex I promote antibiotic persistence through alterations in intracellular acidity and protein synthesis. Nat Commun. 2022;13. doi:10.1038/s41467-022-28141-x
18. Wilmaerts D, Focant C, Matthay P, Michiels J. Transcription-coupled DNA repair underlies variation in persister awakening and the emergence of resistance. Cell Rep. 2022;38. doi:10.1016/j.celrep.2022.110427
19. Dewachter L, Bollen C, Wilmaerts D, Louwagie E, Herpels P, Matthay P, et al. The Dynamic Transition of Persistence toward the Viable but Nonculturable State during Stationary Phase Is Driven by Protein Aggregation. 2021. doi:10.1128/mBio
20. Goode O, Smith A, Łapińska U, Bamford R, Kahveci Z, Glover G, et al. Heterologous Protein Expression Favors the Formation of Protein Aggregates in Persister and Viable but Nonculturable Bacteria. ACS Infect Dis. 2021;7: 1848–1858. doi:10.1021/acsinfecdis.1c00154
21. Sharma B, Brown A v, Matluck NE, Hu LT, Lewis K. Borrelia burgdorferi, the Causative Agent of Lyme Disease, Forms Drug-Tolerant Persister Cells. 2015. doi:10.1128/AAC.00864-15
22. Meyer KJ, Taylor HB, Seidel J, Gates MF, Lewis K. Pulse Dosing of Antibiotic Enhances Killing of a Staphylococcus aureus Biofilm. Front Microbiol. 2020;11. doi:10.3389/fmicb.2020.596227
23. Cooper NG, Julius AA. Bacterial persistence: Mathematical modeling and optimal treatment strategy. Proceedings of the American Control Conference. Institute of Electrical and Electronics Engineers Inc.; 2011. pp. 3502–3507. doi:10.1109/acc.2011.5991194

24. Cogan NG, Brown J, Darres K, Petty K. Optimal control strategies for disinfection of bacterial populations with persister and susceptible dynamics. Antimicrob Agents Chemother. 2012;56: 4816–4826. doi:10.1128/AAC.00675-12
25. Himeoka Y, Mitarai N. When to wake up? The optimal waking-up strategies for starvation-induced persistence. 2019. Available: http://arxiv.org/abs/1912.12682
26. de Leenheer P, Cogan NG. Failure of antibiotic treatment in microbial populations. J Math Biol. 2009;59: 563–579. doi:10.1007/s00285-008-0243-6
27. Imran M, Smith H. A model of optimal dosing of antibiotic treatment in biofilm. Mathematical Biosciences and Engineering. 2014;11: 547–571. doi:10.3934/mbe.2014.11.547
28. Cogan NG, Rath H, Kommerein N, Stumpp SN, Stiesch M. Theoretical and experimental evidence for eliminating persister bacteria by manipulating killing timing. FEMS Microbiol Lett. 2016;363: 1–6. doi:10.1093/femsle/fnw264
29. Michiels JE, van den Bergh B, Verstraeten N, Fauvart M, Michiels J. In vitro emergence of high persistence upon periodic aminoglycoside challenge in the ESKAPE pathogens. Antimicrob Agents Chemother. 2016;60: 4630–4637. doi:10.1128/AAC.00757-16
30. van den Bergh B, Michiels JE, Wenseleers T, Windels EM, Boer P vanden, Kestemont D, et al. Frequency of antibiotic application drives rapid evolutionary adaptation of Escherichia coli persistence. Nat Microbiol. 2016;1. doi:10.1038/nmicrobiol.2016.20
31. Amato SM, Orman MA, Brynildsen MP. Metabolic Control of Persister Formation in Escherichia coli. Mol Cell. 2013. doi:10.1016/j.molcel.2013.04.002
32. Orman MA, Brynildsen MP. Inhibition of stationary phase respiration impairs persister formation in E. coli. Nat Commun. 2015;6. doi:10.1038/ncomms8983
33. Mohiuddin SG, Kavousi P, Orman MA. Flow-cytometry analysis reveals persister resuscitation characteristics. BMC Microbiol. 2020;20. doi:10.1186/s12866-020-01888-3
34. Carvalho G, Guilhen C, Balestrino D, Forestier C, Mathias JD. Relating switching rates between normal and persister cells to substrate and antibiotic concentrations: a mathematical modelling approach supported by experiments. Microb Biotechnol. 2017;10: 1616–1627. doi:10.1111/1751-7915.12739
35. Nikolaou M, Schilling AN, Vo G, Chang KT, Tam VH. Modeling of microbial population responses to time-periodic concentrations of antimicrobial agents. Ann Biomed Eng. 2007;35: 1458–1470. doi:10.1007/s10439-007-9306-x
36. Imran M, Smith H. A model of optimal dosing of antibiotic treatment in biofilm. Mathematical Biosciences and Engineering. 2014;11: 547–571. doi:10.3934/mbe.2014.11.547
37. Craig WA, Middleton WS. Pharmacokinetic/Pharmacodynamic Parameters: Rationale for Antibacterial Dosing of Mice and Men. Clinical Infectious Diseases. 1998. Available: https://academic.oup.com/cid/article/26/1/1/350424
38. Mohiuddin SG, Kavousi P, Orman MA. Flow-cytometry analysis reveals persister resuscitation characteristics. BMC Microbiol. 2020;20. doi:10.1186/s12866-020-01888-3

39. Ayrapetyan M, Williams TC, Oliver JD. Bridging the gap between viable but non-culturable and antibiotic persistent bacteria. Trends in Microbiology. Elsevier Ltd; 2015. pp. 7–13. doi:10.1016/j.tim.2014.09.004
40. Dewachter L, Bollen C, Wilmaerts D, Louwagie E, Herpels P, Matthay P, et al. The Dynamic Transition of Persistence toward the Viable but Nonculturable State during Stationary Phase Is Driven by Protein Aggregation. 2021. doi:10.1128/mBio
41. Bamford RA, Smith A, Metz J, Glover G, Titball RW, Pagliara S. Investigating the physiology of viable but non-culturable bacteria by microfluidics and time-lapse microscopy. BMC Biol. 2017;15. doi:10.1186/s12915-017-0465-4
42. Dong K, Pan H, Yang D, Rao L, Zhao L, Wang Y, et al. Induction, detection, formation, and resuscitation of viable but non-culturable state microorganisms. Compr Rev Food Sci Food Saf. 2020;19: 149–183. doi:10.1111/1541-4337.12513
43. Zhang XH, Ahmad W, Zhu XY, Chen J, Austin B. Viable but nonculturable bacteria and their resuscitation: implications for cultivating uncultured marine microorganisms. Marine Life Science and Technology. Springer; 2021. pp. 189–203. doi:10.1007/s42995-020-00041-3
44. Dong K, Pan H, Yang D, Rao L, Zhao L, Wang Y, et al. Induction, detection, formation, and resuscitation of viable but non-culturable state microorganisms. Compr Rev Food Sci Food Saf. 2020;19: 149–183. doi:10.1111/1541-4337.12513
45. Zhang XH, Ahmad W, Zhu XY, Chen J, Austin B. Viable but nonculturable bacteria and their resuscitation: implications for cultivating uncultured marine microorganisms. Marine Life Science and Technology. Springer; 2021. pp. 189–203. doi:10.1007/s42995-020-00041-3

## 7 SUPPORTING INFORMATION

SI-1APPENDIX A. Derivation of eqn. (7)
SI-2APPENDIX B. Optimal rate of decline for bacterial population peaks characterized by eqn. (9)
SI-3APPENDIX C. Estimation of $K_{n,\mathrm{off}}, K_{n,\mathrm{on}}$ from data in Fig 5
SI-4APPENDIX D. Analytical solution of eqns. (1) and (2)